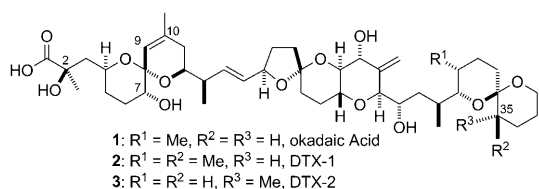


# Total Synthesis of Dinophysistoxin-2 and 2-*epi*-Dinophysistoxin-2 and Their PPase Inhibition\*\*

Yucheng Pang, Chao Fang, Michael J. Twiner, Christopher O. Miles, and Craig J. Forsyth\*

Okadaic acid (OA, **1**) and its analogues—dinophysistoxin-1 (DTX-1, **2**) and -2 (DTX-2, **3**)—accumulated in mussels feeding on certain marine algae species,<sup>[1]</sup> are causative agents of “diarrhetic shellfish poisoning” throughout the world.<sup>[2]</sup> Okadaic acid and naturally occurring biosynthetic variants have demonstrated both potent protein serine-threonine phosphatase (PPase) inhibitory activities and apoptosis-inducing activities among numerous cancerous cell lines.<sup>[3–5]</sup> Circumstantially, these activities appear to be causally related. Thus, elucidating the structural basis of selective and potent OA-type PPase inhibition may underlie the discovery of novel anticancer leads. Herein, we disclose the first total synthesis of **3** and its nonnatural analogue 2-*epi*-**3**, and their PPase inhibitory activities.

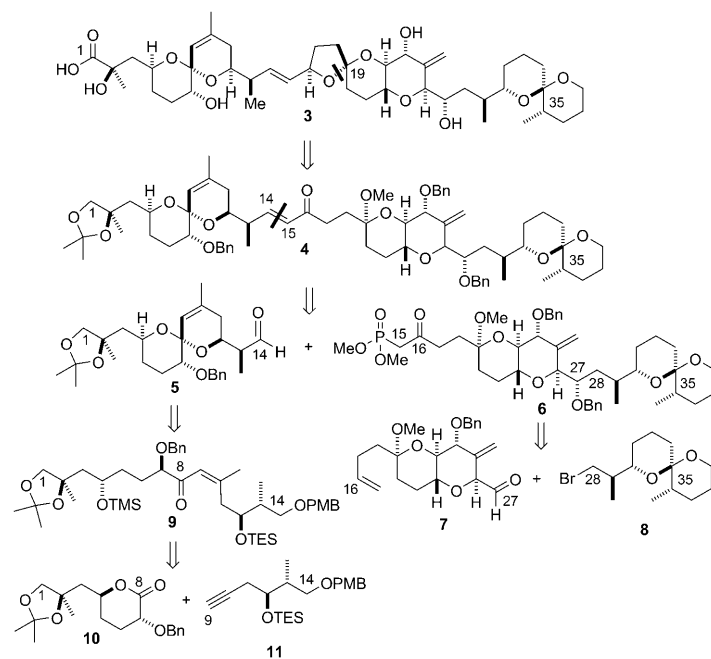


The effect of the stereochemistry of the methyl-bearing carbon 35 of **2** and **3** on PPase inhibitory activity has recently been described.<sup>[5]</sup> Compared to **1** and **2**, **3** was found to be a weaker inhibitor of PP2A.<sup>[4,5]</sup> Thus, variable functionalization at both the C1–C2 region and the C30–C38 domain confers differential PPase inhibitory activities. Some structural modifications about the C1–C14 domain of **1** have been shown to be tolerated (e.g. 7-deoxy,<sup>[6]</sup> C9,10-episulfide<sup>[7]</sup>), whereas others are not (2-deoxy, 2-oxo decarboxylate, and methyl

ester at C1)<sup>[6]</sup> with respect to retaining appreciable PPase activity. Herein, we show that the configuration at C2 of **3** also has a dramatic effect on PPase inhibitory activity.

The synthetic design of **3** featured reliable fragment coupling methods derived from our previous study of **1**,<sup>[8b]</sup> but also highlights novel approaches to assemble the C1–C14 and C28–C38 domains. As a result, the overall efficiency of the assembly of **3** more than doubles that previously established for **1**.<sup>[8]</sup> Specifically, **1** was prepared in 1.7% overall yield spanning 26 steps in the longest linear sequence,<sup>[8b]</sup> whereas **3** is delivered in 3.6% yield over 21 steps by the approach outlined herein.

The natural product **3** was designed to derive from enone **4** through a late-stage installation of the spiroketal at C19 by a reduction/transketalization sequence (Scheme 1).<sup>[8b,9]</sup> The two key intermediates, C1–C14 aldehyde **5** and C15–C38 β-keto phosphonate **6**, could be coupled through a Horner–Wadsworth–Emmons reaction. The spiroketal at C8 in **5** could be established upon treatment of enone **9** with acid. In turn, **9** could be derived from the opening of lactone **10**<sup>[10]</sup> with the acetylide derived from alkyne **11**. The C15–C38 domain was dissected at the C27–28 bond into aldehyde **7** and bromide **8**. Aldehyde **7** represents the central core of **1–3**, whereas **8** is unique to **3** in its methyl substitution at C35.



**Scheme 1.** Retrosynthetic disconnections of DTX-2 (**3**). Bn = benzyl, PMB = *para*-methoxyphenyl, TES = triethylsilyl.

[\*] Y. Pang, C. Fang, Prof. C. J. Forsyth

Department of Chemistry, The Ohio State University  
 100 W. 18th Ave., Columbus, OH 43210 (USA)  
 E-mail: forsyth@chemistry.ohio-state.edu

Prof. M. J. Twiner

Department of Natural Sciences  
 The University of Michigan-Dearborn  
 4901 Evergreen Rd., Dearborn, Michigan 48128 (USA)

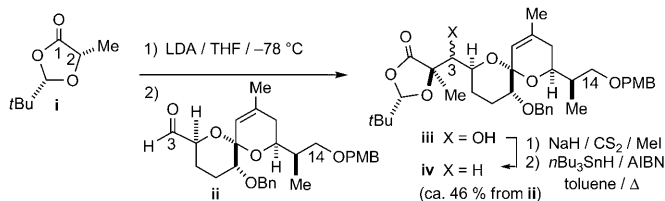
Dr. C. O. Miles  
 Norwegian Veterinary Institute, Chemistry Section  
 PB 750 Sentrum, NO-0106 Oslo (Norway)

[\*\*] We acknowledge the Ohio State University for financial support, Dr. T. Young and A.-K. Yassine for technical help, the Ohio BioProduct Innovation Consortium for mass spectrometry support, and Prof. J. Stambuli for helpful discussion.



Supporting information for this article is available on the WWW under <http://dx.doi.org/10.1002/anie.201101741>.

Our original synthesis of **1** utilized Seebach's lactate pivalidene acetal (**i**) as the source of the C1–C2  $\alpha$ -hydroxy,  $\alpha$ -methyl carboxylic acid (Scheme 2).<sup>[8b,11]</sup> Attempts to imbed this moiety within the okadaic acid intermediate **iv** through late-stage alkylation at C2 of the lactate pivalidene enolate with C3 halides or sulfonates were uniformly unsuccessful. Instead, an aldol reaction was used with a C3 aldehyde (**ii**) for C2–C3 bond formation. The facial selectivity of enolate addition was modest (2:1) and a subsequent Barton deoxygenation of the C3 alcohols (**iii**) was required to complete the task. Thus, the combined yield was about 46% for the formation of C1–C14 intermediate **iv** from **i** and **ii**.

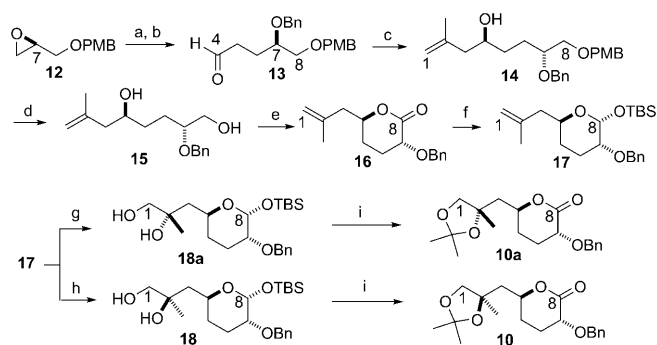


**Scheme 2.** Previous synthesis of the C1–C14 domain of **1**.<sup>[8b]</sup> AIBN = 2,2'-azobisisobutyronitrile, LDA = lithium diisopropylamide, THF = tetrahydrofuran.

An alternative strategy was adopted for the early incorporation of the  $\alpha$ -hydroxy,  $\alpha$ -methyl carboxylate moiety in **3**. This approach involved targeting lactone **10** (Scheme 1), the masked vicinal diol of which could be ultimately oxidized into the  $\alpha$ -hydroxy carboxylic acid of **3**. In the seminal total synthesis of **1**, Isobe et al. installed the core vicinal diol of **10** through a substrate chelation-controlled hydroxymercuration process using a C2–C3 alkene.<sup>[10]</sup> Since then, reagent-controlled Sharpless asymmetric dihydroxylation (SAD) has been well-established to provide reliable and empirically predictable facial selective vicinal dihydroxylations of alkenes.<sup>[12]</sup> We aimed to apply the SAD process with the C1–C2 alkene of **17** en route to **10**, which in turn would serve as a precursor to the C1–C14 domain **5**. However, an unexpected outcome was obtained.

The synthesis of **10** began with conversion of epoxide **12**<sup>[13]</sup> into aldehyde **13** (Scheme 3). Keck methallylation<sup>[14]</sup> of **13** installed the stereogenic center at C4 of **3** in homoallylic alcohol **14**. The PMB ether of **14** was cleaved to generate 1,5-diol **15**, which was oxidatively lactonized to **16** with TEMPO and BAIB.<sup>[15]</sup> The SAD process was originally applied to **16** but undesired saponification occurred under the basic AD-mix conditions. Alternatively, lactone **16** was converted into mixed acetal **17** through a reduction/silylation sequence.

Application of AD-mix- $\beta$ <sup>[12a]</sup> dihydroxylation to **17** generated the vicinal primary/tertiary diol **18a** in 9:1 diastereoselectivity. It was anticipated that diol **18** would be the major diastereomer according to Sharpless' empirical rules<sup>[12]</sup> and most previous applications of SAD with terminal unsymmetrical disubstituted alkenes.<sup>[12a,16]</sup> However, after converting the major diol diastereomer **18a** into the corresponding  $\delta$ -lactone **10a** it was found that the SAD reaction had given the opposite diastereoselectivity. This was determined by com-



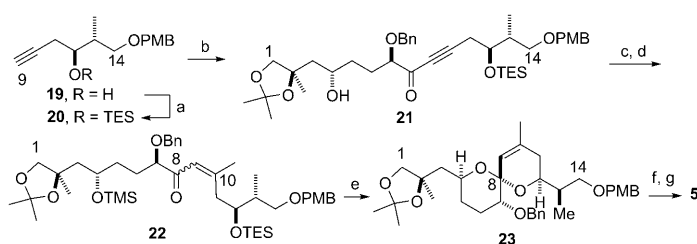
**Scheme 3.** Synthesis of lactone **10**. Reagents and conditions:

a) allylMgBr, CuI (cat.), THF,  $-40^{\circ}\text{C}$ , then NaH, THF, BnBr, TBAI; b)  $\text{O}_3$ ,  $\text{CH}_2\text{Cl}_2$ ,  $\text{CH}_3\text{OH}$ ,  $-78^{\circ}\text{C}$ ; then  $\text{PPh}_3$ , 70% (2 steps); c) tributyl(2-methylallyl)stannane, (+)-binol,  $\text{Ti}(\text{O}i\text{Pr})_4$ ,  $\text{CH}_2\text{Cl}_2$ , molecular sieves (4 Å),  $-20^{\circ}\text{C}$ , 99%, d.r. = 6:1; d) DDQ,  $t\text{BuOH}$ , pH 7 buffer,  $\text{CH}_2\text{Cl}_2$ , 80%; e) TEMPO, BAIB,  $\text{CH}_2\text{Cl}_2$ , 83%; f) DIBAL,  $\text{CH}_2\text{Cl}_2$ ,  $-78^{\circ}\text{C}$  to  $40^{\circ}\text{C}$ , then TBSCl, imidazole, DMAP,  $\text{CH}_2\text{Cl}_2$ , 99%. g) AD-mix- $\beta$ ,  $t\text{BuOH}$ ,  $\text{H}_2\text{O}$ ,  $0^{\circ}\text{C}$ , d.r. = 9:1, 92%; h) AD-mix- $\alpha$ ,  $t\text{BuOH}$ ,  $\text{H}_2\text{O}$ ,  $0^{\circ}\text{C}$ , d.r. = 3:1, 91%; i) PPTS,  $\text{CH}_2\text{Cl}_2$ , 2,2-dimethoxypropane; then TBAF, THF; then TEMPO, BAIB,  $\text{NaHCO}_3$ ,  $\text{CH}_2\text{Cl}_2$ , 88%. BAIB = iodobenzene diacetate, binol = 1,1'-bi-2-naphthol, DDQ = 2,3-dichloro-5,6-dicyano-1,4-benzoquinone, DIBAL = diisobutylaluminum hydride, DMAP = 4-dimethylaminopyridine, PPTS = pyridinium *p*-toluenesulfonate, TBAF = tetra-*n*-butylammonium fluoride, TBAI = tetra-*n*-butylammonium iodide, TBS = *tert*-butyldimethyl, TEMPO = 2,2,6,6-tetramethylpiperidine-1-oxyl.

parison of spectroscopic data with those obtained previously by Isobe and co-workers<sup>[17]</sup> The SAD was repeated with **17** but using AD-mix- $\alpha$ , which inverted the sense of diastereoselectivity to give a 3:1 diastereomeric ratio of diols **18** and **18a**, respectively. The major diastereomer was converted into a lactone (**10**) as before (Scheme 3). As a control reaction to probe potential inherent substrate bias, dihydroxylation of **17** using  $\text{OsO}_4$  and pyridine/NMO in THF/ $\text{H}_2\text{O}$  gave a 1:1 ratio of diastereomeric diols in good yield.

The differential levels of diastereoselectivity with **17** and AD-mix- $\alpha$  versus AD-mix- $\beta$  may represent mismatched versus matched diastereomeric transition states involving the pseudoenantiomeric AD-mix ligands dihydroquinine and dihydroquinidine, respectively. The unexpected sense of diastereoselectivity in the SAD of **17** can be ascribed to the homoallylic trisubstituted oxane moiety, which reverses the  $\pi$ -facial selectivity generally predicted by the Sharpless empirical model for the AD-mix reagents. These results provide a caveat to the Sharpless' empirical rules<sup>[12]</sup> for the SAD facial selectivity with **17** and perhaps additional olefins of its type. Hale et al. had reported modest levels of anomalous enantioselectivity in the SAD of achiral 1,1-disubstituted methallyl alcohol derivatives.<sup>[11]</sup>

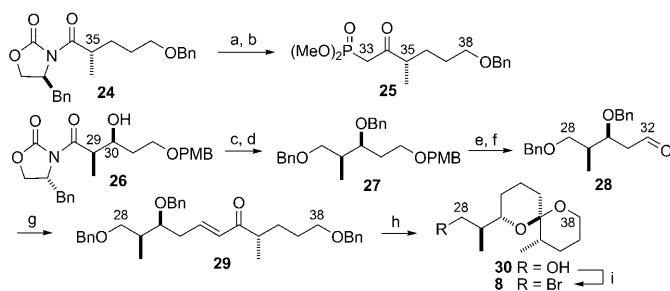
The newly devised synthesis of the C1–C14 domain **5** continued with opening of lactone **10** with the lithium acetylide generated from **19**<sup>[8b]</sup> to give ynone **21** (Scheme 4). After silylation of the residual alcohol, conjugate addition of methylcuprate afforded an *E/Z* mixture of enones **22**. Cleavage of the silyl ether groups and spiroketalization using PPTS in  $\text{CH}_2\text{Cl}_2$  and methanol yielded thermodynamically favored **23**. To complete the synthesis of **5**, the PMB ether of **23** was



**Scheme 4.** Synthesis of aldehyde **5**. Reagents and conditions: a) TESCl, imidazole, DMAP, CH<sub>2</sub>Cl<sub>2</sub>, 99%; b) *n*BuLi, THF, –78 °C; then **10**, 95%; c) TMSCl, imidazole, CH<sub>2</sub>Cl<sub>2</sub>; d) MeLi, CuI, Et<sub>2</sub>O, –40 °C; e) PPTS, CH<sub>2</sub>Cl<sub>2</sub>, MeOH, 38% (3 steps); f) DDQ, *t*BuOH, H<sub>2</sub>O, pH 7 buffer; g) DMP, NaHCO<sub>3</sub>, CH<sub>2</sub>Cl<sub>2</sub>, 82% (2 steps). DMP = Dess–Martin periodinane, TMS = trimethylsilyl.

oxidatively cleaved and the resultant primary alcohol was oxidized using the Dess–Martin periodinane reagent.<sup>[18]</sup> This preparation of the C1–C14 domain of **1–3** is unprecedented in its overall efficiency (8.0% overall yield over 15 steps from **12**).

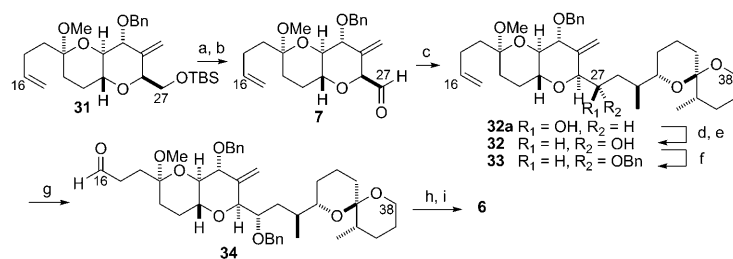
The synthesis of the C15–C38 domain **6** relied upon generation of the common central C15–C27 intermediate **7** and the unique C28–C38 bromide **8**. The newly developed synthesis of the C30–C40 terminal spiroketal domain of **3** necessarily deviated from that previously used for **1**. Although a Keck crotylation was used to set the configurations at vicinal C30 and C31 stereogenic centers in our original synthesis of **1**,<sup>[8b]</sup> the stereogenic centers at C29, C30, and C35 in **3** were established reliably by Evans asymmetric aldol and alkylation processes. Imide **24**<sup>[19]</sup> provided access to the C33–C38 phosphonate **25**, and the complementary C28–C32 aldehyde **28** was obtained from aldol adduct **26**<sup>[20]</sup> (Scheme 5). Reduction of **26** afforded a diol that was protected as dibenzyl ether **27**. The PMB ether of **27** was selectively cleaved and the resultant alcohol was oxidized to aldehyde **28**. β-Ketophosphonate **25** was then coupled with **28**.<sup>[21]</sup> The resulting enone **29** was converted into the thermodynamically favored spiroketal **30** in a single process. Hydrogenation of **29** using Pearlman's catalyst in ethanol saturated the alkene, cleaved the three benzyl ethers, and



**Scheme 5.** Synthesis of bromide **8**. Reagents and conditions: a) MeMgBr, MeOH, 0 °C; b) dimethyl methylphosphonate, *n*BuLi, THF, –78 °C, 76% (2 steps); c) NaBH<sub>4</sub>, THF, H<sub>2</sub>O; d) NaH, BnBr, TBAI, THF, 67% (2 steps); e) DDQ, *t*BuOH, pH 7 buffer, CH<sub>2</sub>Cl<sub>2</sub>; f) py-SO<sub>3</sub>, DMSO, *i*Pr<sub>2</sub>NEt, CH<sub>2</sub>Cl<sub>2</sub>, 87% (2 steps); g) **25**, LiCl, *i*Pr<sub>2</sub>NEt, CH<sub>3</sub>CN, 97%; h) H<sub>2</sub>, Pd(OH)<sub>2</sub>/C, EtOH, 93%; i) CBr<sub>4</sub>, PPh<sub>3</sub>, Et<sub>3</sub>N, CH<sub>2</sub>Cl<sub>2</sub>, 95%. DMSO = dimethyl sulfoxide, py = pyridine.

dehydratively spiroketalized the in situ generated keto triol to **30** in 93% yield of isolated product. Thereafter, the residual alcohol was converted into bromide **8**.<sup>[22]</sup>

The C16–C27 aldehyde **7**, prepared from **31**,<sup>[23]</sup> was coupled with the alkyl lithium derived from **8** (Scheme 6).<sup>[24]</sup> The resultant mixture of epimeric alcohols **32a** and **32** were separated and **32a** was converted into **32** through oxidation/reduction.<sup>[8a,d]</sup> After benzylation of alcohol **32**, the less-hindered alkene in **33** was oxidized to aldehyde **34** by treatment with OsO<sub>4</sub> and NaIO<sub>4</sub>.<sup>[23]</sup> A sequence of phosphonate anion addition and oxidation using Dess–Martin periodinane converted **34** into β-ketophosphonate **6**.

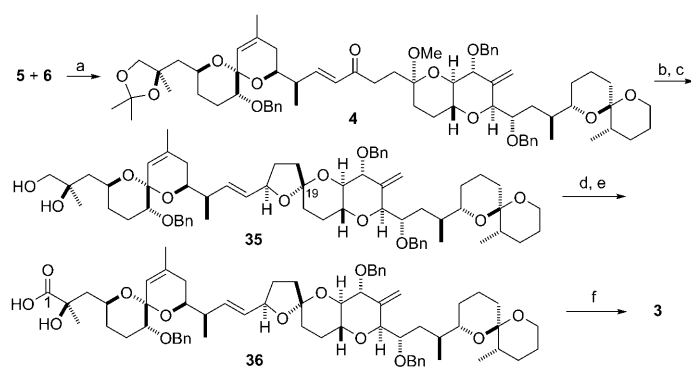


**Scheme 6.** Synthesis of **6**. Reagents and conditions: a) TBAF, THF, 100%; b) DMP, NaHCO<sub>3</sub>, CH<sub>2</sub>Cl<sub>2</sub>; c) **8**, *t*BuLi, Et<sub>2</sub>O –78 °C to 25 °C; then **7**, –78 °C, 48%, d.r. = 1:1; d) DMP, NaHCO<sub>3</sub>, CH<sub>2</sub>Cl<sub>2</sub>; e) NaBH<sub>4</sub>, MeOH, –20 °C, 90% (2 steps); f) NaH, THF; then BnBr, TBAI, 93%; g) OsO<sub>4</sub>, NaIO<sub>4</sub>, THF, H<sub>2</sub>O, 77%; h) dimethyl methylphosphonate, *t*BuLi, THF, –78 °C; i) DMP, NaHCO<sub>3</sub>, CH<sub>2</sub>Cl<sub>2</sub>, 70% (2 steps).

Only six steps from **5** and **6** were required to complete the first total synthesis of **3**. First, aldehyde **5** and β-ketophosphonate **6** were coupled in high yield to give (*E*)-enone **4** (Scheme 6). Diastereoselective reduction of the ketone using (*S*)-CBS catalyst<sup>[25]</sup> converted **4** into the (16*R*)-alcohol, which upon treatment with acetic acid in THF and water underwent intramolecular transketalization and acetonide hydrolysis to yield diol **35** (Scheme 7). Sequential Parikh–Doering<sup>[26]</sup> and Pinnick<sup>[27]</sup> oxidations converted **35** into α-hydroxy acid **36**.

Finally, the three benzyl groups were cleaved in THF at –78 °C using freshly prepared LiDBB<sup>[28]</sup> to provide **3**. Moreover, 2-*epi*-DTX-2 was also prepared in the same fashion as **3** by replacing **10** with **10a** in the synthetic sequence. Confirmation of the identity of synthetic **3** with naturally occurring DTX2 was obtained by comparison of LC-HRMS and <sup>1</sup>H NMR data.<sup>[29]</sup>

Naturally isolated **1** and **3**<sup>[30]</sup> were tested in parallel with synthetic **3** and 2-*epi*-**3** for their PP2A and PP1 inhibition activity. All toxins were shown to inhibit each of these enzymes but with various degrees of potency (Figure 1). Although PP2A was always more sensitive than PP1, the relative order of potency of the toxins remained the same for both enzymes: nat. **1** > nat. **3** ≈ synthetic **3** > synthetic 2-*epi*-**3**. Respective IC<sub>50</sub> values (nM) for PP2A are 0.47, 0.99, 1.35, and 137, and for PP1 are 25.2, 76.4, 82.6, and 3114 (Table 1 in the Supporting Information). The IC<sub>50</sub> value for **1** on PP2A and PP1 is



**Scheme 7.** Total synthesis of **3**. Reagents and conditions: a) LiCl, *i*Pr<sub>2</sub>NEt, CH<sub>3</sub>CN, 93%; b) (*S*)-Me-CBS, BH<sub>3</sub>·THF, THF, 0 °C; c) AcOH, THF, H<sub>2</sub>O, 55 °C, 36 h, 80%; d) py-SO<sub>3</sub>, DMSO, *i*Pr<sub>2</sub>NEt, CH<sub>2</sub>Cl<sub>2</sub>; e) NaClO<sub>2</sub>, NaH<sub>2</sub>PO<sub>4</sub>, 2-methyl-2-butene, *t*BuOH, H<sub>2</sub>O, 0 °C, 89%; f) LiDBB, THF, -78 °C, 69%. DBB = 4,4'-di-*tert*-butylbiphenyl, (*S*)-Me-CBS = Corey–Bakshi–Shibata oxaborolidine.

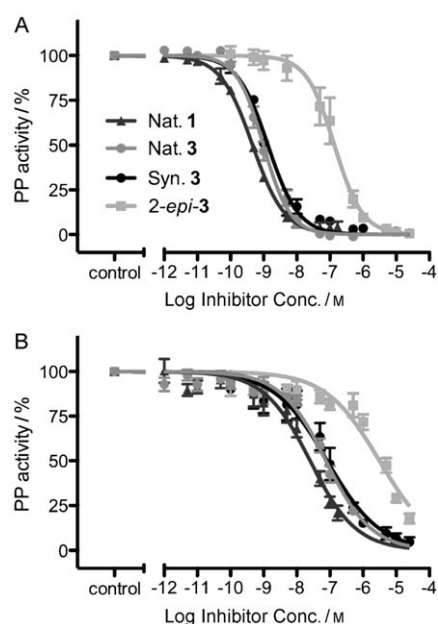


**Figure 1.** Inhibitory effects of natural OA (**1**), natural and synthetic DTX-2 (**3**), and synthetic 2-*epi*-DTX-2 on (A) PP2A and (B) PP1 activity.

within the range of other published reports,<sup>[5b,6,31]</sup> as is the IC<sub>50</sub> value for **3** (both natural and synthetic) on PP2A (3.5 nM).<sup>[32]</sup>

These studies indicate that the nonnatural synthetic analogue 2-*epi*-**3** is at least 1 to 2 orders of magnitude less potent than **3** (101- and 38-fold for PP2A and PP1, respectively). The fact that the C2 epimer of DTX2 has such a remarkably decreased potency (IC<sub>50</sub> = 137 and 3114 nM for PP2A and PP1, respectively) indicates biogenetic optimization of PPase inhibitory activity and the essential roles of detailed structural features within the C1–C12 domain for conferring biological activity of okadaic acid and its congeners.<sup>[6]</sup>

The structural basis for the differential PPase inhibition by **3** and 2-*epi*-**3** may involve docking of both compounds at

the active sites of the respective enzymes in either similar or considerably different conformations. For the former, the hydroxy and methyl substituents at C2 of **3** and 2-*epi*-**3** would be projected in opposite directions. For 2-*epi*-**3** this may cause the loss of potentially favorable contacts between the hydroxyl group at C2 and Tyr272 and Arg96, and between the methyl group at C2 and His125 in PP1.<sup>[33]</sup> Similar disruption of hydrogen bonding contacts between the hydroxyl group at C2 and Tyr265 and Arg89 in PP2A may occur.<sup>[32]</sup> The marriage of novel fragment assemblies with reliably established tricomponent couplings described here will provide access to further structural analogues derived from both **3** and the novel nonnatural analogue 2-*epi*-**3**. These unique molecules will facilitate studies to further elucidate the structural basis of selective PPase regulation and associated biological consequences.

Received: March 10, 2011

Revised: May 27, 2011

Published online: July 1, 2011

**Keywords:** natural products · phosphatase inhibitors · structure–activity relationships · total synthesis

- [1] a) K. Tachibana, P. J. Scheuer, Y. Tsukitani, H. Kikuchi, D. Van Engen, J. Clardy, Y. Gopichand, F. J. Schmitz, *J. Am. Chem. Soc.* **1981**, *103*, 2469–2471; b) M. Murata, M. Shimatani, H. Sugitani, Y. Oshima, T. Yasumoto, *Bull. Jpn. Soc. Sci. Fish.* **1982**, *48*, 549–552; c) T. Hu, J. Doyle, D. Jackson, J. Marr, E. Nixon, S. Pleasance, M. A. Quilliam, J. A. Walter, J. L. C. Wright, *J. Chem. Soc. Chem. Commun.* **1992**, 39–41.
- [2] C. F. B. Holmes, H. A. Luu, F. Carrier, F. J. Schmitz, *FEBS Lett.* **1990**, *270*, 216–218.
- [3] T. Yasumoto, M. Murata, *Chem. Rev.* **1993**, *93*, 1897–1909.
- [4] T. Aune, S. Larsen, J. A. B. Aasen, N. Rehmman, M. Satake, P. Hess, *Toxicol.* **2007**, *49*, 1–7.
- [5] a) K. Larsen, D. Petersen, A. L. Wilkins, I. A. Samdal, M. Sandvik, T. Rundberget, D. Goldstone, V. Arcus, P. Hovgaard, F. Rise, N. Rehmman, P. Hess, C. O. Miles, *Chem. Res. Toxicol.* **2007**, *20*, 868–875; b) J. Huhn, P. D. Jeffrey, K. Larsen, T. Rundberget, F. Rise, N. R. Cox, V. Arcus, Y. Shi, C. O. Miles, *Chem. Res. Toxicol.* **2009**, *22*, 1782–1786.
- [6] A. Takai, M. Murata, K. Torigoe, M. Isobe, G. Mieskes, T. Yasumoto, *Biochem. J.* **1992**, *284*, 539–544.
- [7] F. J. Schmitz, R. S. Prasad, Y. Gopichand, M. B. Hossain, D. van der Helm, P. Schmidt, *J. Am. Chem. Soc.* **1981**, *103*, 2467–2469.
- [8] a) M. Isobe, Y. Ichikawa, D. L. Bai, H. Masaki, T. Goto, *Tetrahedron* **1987**, *43*, 4767–4776; b) C. J. Forsyth, S. F. Sabes, R. A. Urbanek, *J. Am. Chem. Soc.* **1997**, *119*, 8381–8382; c) S. F. Sabes, R. A. Urbanek, C. J. Forsyth, *J. Am. Chem. Soc.* **1998**, *120*, 2534–2542; d) R. A. Urbanek, S. F. Sabes, C. J. Forsyth, *J. Am. Chem. Soc.* **1998**, *120*, 2523–2533; e) S. V. Ley, A. C. Humphries, H. Eick, R. Downham, A. R. Ross, R. J. Boyce, J. B. J. Pavey, J. Pietruszka, *J. Chem. Soc. Perkin Trans. 1* **1998**, 3907–3911.
- [9] A. B. Dounay, R. A. Urbanek, S. F. Sabes, C. J. Forsyth, *Angew. Chem.* **1999**, *111*, 2403–2406; *Angew. Chem. Int. Ed.* **1999**, *38*, 2258–2262.
- [10] Compound **10** was previously prepared by Isobe using an oxymercuration/demercuration protocol to set the tertiary stereogenic center: M. Isobe, Y. Ichikawa, T. Goto, *Tetrahedron Lett.* **1986**, *26*, 5199–5202.

- [11] K. F. Hale, S. Manaviazar, S. A. Peak, *Tetrahedron Lett.* **1994**, 35, 425–428.
- [12] a) H. C. Kolb, M. S. VanNieuwenhuz, K. B. Sharpless, *Chem. Rev.* **1994**, 94, 2483–2547; b) K. B. Sharpless, W. Amberg, Y. L. Bennani, G. A. Crispino, J. Hartung, K. S. Jeong, H.-L. Kwong, K. Morikawa, Z.-M. Wang, D. Xu, X.-L. Zhang, *J. Org. Chem.* **1992**, 57, 2768–2771.
- [13] M. E. Furrow, S. E. Schaus, E. N. Jacobsen, *J. Org. Chem.* **1998**, 63, 6776–6777.
- [14] G. E. Keck, K. H. Tarbet, L. S. Gareci, *J. Am. Chem. Soc.* **1993**, 115, 8467–8468.
- [15] T. M. Hansen, G. J. Florence, P. Lugo-Mas, J. Chen, J. N. Abrams, C. J. Forsyth, *Tetrahedron Lett.* **2003**, 44, 57–59.
- [16] A. B. Smith III, C. Sfougataki, C. A. Risatti, J. B. Sperry, W. Zhu, V. A. Doughty, T. Tomioka, D. B. Gotchev, C. S. Bennett, S. Sakamoto, O. Atasoylu, S. Shirakami, D. Bauer, M. Takeuchi, J. Koyanagi, Y. Sakamoto, *Tetrahedron* **2009**, 65, 6489–6509.
- [17] Y. Ichikawa, M. Isobe, D. L. Bai, T. Goto, *Tetrahedron* **1987**, 43, 4737–4748.
- [18] D. B. Dess, J. C. Martin, *J. Org. Chem.* **1983**, 48, 4155–4156.
- [19] K. H. Altmann, G. Bold, G. Caravatti, D. Denni, A. Florsheimer, A. Schmidt, G. Rihs, M. Wartmann, *Helv. Chim. Acta* **2002**, 85, 4086–4110.
- [20] L. C. Dias, S. M. Pinheiro, V. M. de Oliveira, M. A. B. Ferreira, C. F. Tormena, A. M. Aguilar, J. Zukerman-Schpector, E. R. T. Tiekink, *Tetrahedron* **2009**, 65, 8714–8721.
- [21] M. A. Blanchette, W. Choy, J. T. Davis, A. P. Essensfeld, S. Masamune, W. R. Roush, T. Sakai, *Tetrahedron Lett.* **1984**, 25, 2183–2186.
- [22] R. Appel, *Angew. Chem.* **1975**, 87, 863–874; *Angew. Chem. Int. Ed. Engl.* **1975**, 14, 801–811.
- [23] A. B. Dounay, R. A. Urbanek, V. A. Frydrychowski, C. J. Forsyth, *J. Org. Chem.* **2001**, 66, 925–938.
- [24] C. Fang, Y. Pang, C. J. Forsyth, *Org. Lett.* **2010**, 12, 4528–4531.
- [25] E. J. Corey, R. K. Bakshi, S. Shibata, C. P. Chen, V. K. Singh, *J. Am. Chem. Soc.* **1987**, 109, 7925–7926.
- [26] J. R. Parikh, W. v. E. Doering, *J. Am. Chem. Soc.* **1967**, 89, 5505–5507.
- [27] B. S. Bal, W. E. Childers, Jr., H. W. Pinnick, *Tetrahedron* **1981**, 37, 2091–2096.
- [28] P. K. Freeman, L. L. Hutchinson, *J. Org. Chem.* **1980**, 45, 1924–1930.
- [29] See the Supporting Information.
- [30] A sample of naturally occurring DTX2 was obtained from the National Research Council (Canada).
- [31] C. Bialojan, A. Takai, *Biochem. J.* **1998**, 256, 283–290.
- [32] Y. Xing, Y. Xu, Y. Chen, P. D. Jeffrey, Y. Chao, Z. Lin, Z. Li, S. Strack, J. B. Stock, Y. Shi, *Cell* **2006**, 127, 341–353.
- [33] J. T. Maynes, K. S. Bateman, M. M. Cherney, A. K. Das, H. A. Luu, C. F. B. Holmes, M. N. G. James, *J. Biol. Chem.* **2001**, 276, 44078–44882.